High-mass X-ray Binaries: Illuminating the Passage from Massive Binaries to Merging Compact Objects
Proceedings IAU Symposium No. 346, 2019
L. M. Oskinova, E. Bozzo, T. Bulik & D. Gies, eds.

doi:10.1017/S1743921318008438

Massive star mass-loss revealed by X-ray observations of young supernovae

Vikram V. Dwarkadas

Dept. of Astronomy and Astrophysics, Univ of Chicago
5640 S Ellis Ave, Chicago, IL 60637
email: vikram@astro.uchicago.edu

Abstract. Massive stars lose a considerable amount of mass during their lifetime. When the star explodes as a supernova (SN), the resulting shock wave expands in the medium created by the stellar mass-loss. Thermal X-ray emission from the SN depends on the square of the density of the ambient medium, which in turn depends on the mass-loss rate (and velocity) of the progenitor wind. The emission can therefore be used to probe the stellar mass-loss in the decades or centuries before the star's death.

We have aggregated together data available in the literature, or analysed by us, to compute the X-ray lightcurves of almost all young supernovae detectable in X-rays. We use this database to explore the mass-loss rates of massive stars that collapse to form supernovae. Mass-loss rates are lowest for the common Type IIP supernovae, but increase by several orders of magnitude for the highest luminosity X-ray SNe.

Keywords. radiation mechanisms: thermal; shock waves; astronomical data bases: miscellaneous; circumstellar matter; stars: mass loss; supernovae: general; stars: winds, outflows; stars: Wolf-Rayet; X-rays: general

1. Introduction

Core-collapse Supernovae (SNe) arise from massive stars. These stars have strong mass-loss in the form of stellar winds, with mass-loss rates ranging from 10^{-7} to 10^{-4} $M_\odot$ yr^{-1}, and therefore lose a considerable amount of mass over their evolution. When the SN explodes, the resulting shock wave expands in this wind-blown medium. The evolution of the SN shock wave, and the resulting emission, depends on the structure and density profile of this medium. The radiation signatures from the expansion of the SN shock wave can be used to trace the density profile of this medium, which is formed by pre-supernova wind mass-loss. Since the shock wave heats the gas to high temperatures, X-ray emission is one of the signposts of the shock wave interaction with the circumstellar medium (Chevalier & Fransson 2003)

2. X-Ray Emission

X-ray emission from young SNe has been found to be both thermal and non-thermal. If the X-ray emission from the SN is thermal, due to thermal bremsstrahlung with line emission, the X-ray luminosity of the SN shock wave can be written as (Chevalier & Fransson 2003):

$$L_i = 3 \times 10^{39} g_{ff} C_n \left(\frac{\dot{M}_{-5}}{v_{w10}}\right)^2 \left(\frac{t}{10\,\mathrm{d}}\right)^{-1} \mathrm{ergs\ s^{-1}} \tag{2.1}$$

where i can refer to either the forward or reverse shock, g_{ff} is the Gaunt factor, $C_n = 1$ for the circumstellar shock and $(n-3)(n-4)^2/4(n-2)$ for the reverse shock. $\dot{M}_{-5}$ is the mass-loss rate of the wind into which the SN is expanding, in units of 10^{-5} $M_\odot$ yr^{-1}, v_{w10} is the wind velocity in units of 10 km s^{-1}, and t is the time in days. The mass-loss rate and wind velocity are assumed constant, leading to a density in the wind medium that decreases as r^{-2}, and an X-ray luminosity decreasing as t^{-1}. Note that the X-ray luminosity implied by this equation is technically the luminosity over the entire X-ray range, while current X-ray satellites such as *Chandra*, *XMM-Newton* and *Swift* are only effective in a limited X-ray range of around 0.5-10 keV. Electron-ion equilibration behind the shock front is assumed, which is probably not true for young SNe except when the density is very high. However the equation can be easily modified to account for any specified ratio of electron to ion temperature.

2.1. *X-Ray Spectra of SNe*

Inspection of the X-ray spectra can reveal whether the emission is thermal or non-thermal. A non-thermal spectrum would resemble a power-law. Although it appears simple to distinguish between them in principle, in practice it is much more difficult, due to low counts, and the fact that it is possible some may have both a thermal and non-thermal emission component. Nevertheless, some general points can be made, keeping in mind that due to the small statistics, exceptions are always possible.

• *Type IIn SNe* Observed Type IIn spectra are clearly thermal, showing distinct lines of various elements, especially α elements. All IIns that have been observed in X-rays thus far (Bauer *et al.* 2008, Chandra *et al.* 2009, Chandra *et al.* 2012, Chandra *et al.* 2015, Dwarkadas *et al.* 2016) display thermal spectra. Chandra *et al.* (2015) tried to invoke a non-thermal component for SN 2010jl but did not get it to fit.

• *Type Ib/c SNe* Chevalier & Fransson (2006) have suggested that Type Ib/c SNe have X-ray emission that is non-thermal, either inverse Compton or synchrotron.

• *Type IIb SNe* The prototype Type IIb SN, SN 1993J, shows a clearly thermal X-ray spectrum, with distinct lines (Chandra *et al.* 2009, Dwarkadas *et al.* 2014). However Chevalier & Soderberg (2010) have suggested that there is another class of Type IIb SNe with compact progenitors, whose X-ray emission may be non-thermal. The counts for SNe observed in the latter category are generally low, and it has not been easy to categorize the emission mechanism.

• *Type IIL SNe* There are not too many observations of Type IIL SNe in X-rays. SN 1979C was a IIL whose spectrum was fitted with two components. One component was definitely a thermal plasma, while the other could be thermal (Immler *et al.* 2005) or nonthermal (Patnaude *et al.* 2011).

• *Type IIP SNe* The emission from Type IIP was proposed by Chevalier, Fransson & Nymark (2006) to be non-thermal. This was found to be the case for SN 2011ja (Chakraborti *et al.* 2013) and SN 2013ej (Chakraborti *et al.* 2016).

3. X-Ray Lightcurves

Analysis of an X-ray observation of a SN provides a source flux and luminosity at a given epoch. Plotting the luminosity over a series of epochs gives rise to the X-ray lightcurve of the SN. Over the years we have compiled together a library of X-ray lightcurves of young SNe, both those that have appeared in the literature and those analysed by us. This process started with the publication of a first compilation of lightcurves in 2012 (Dwarkadas & Gruszko 2012), to which we have gradually added more over the years (Dwarkadas 2014 and Dwarkadas *et al.* 2016.) Many of these lightcurves are available in an online database that we have created for this purpose (Ross & Dwarkadas 2017), which can be viewed at kronos.uchicago.edu/snax.

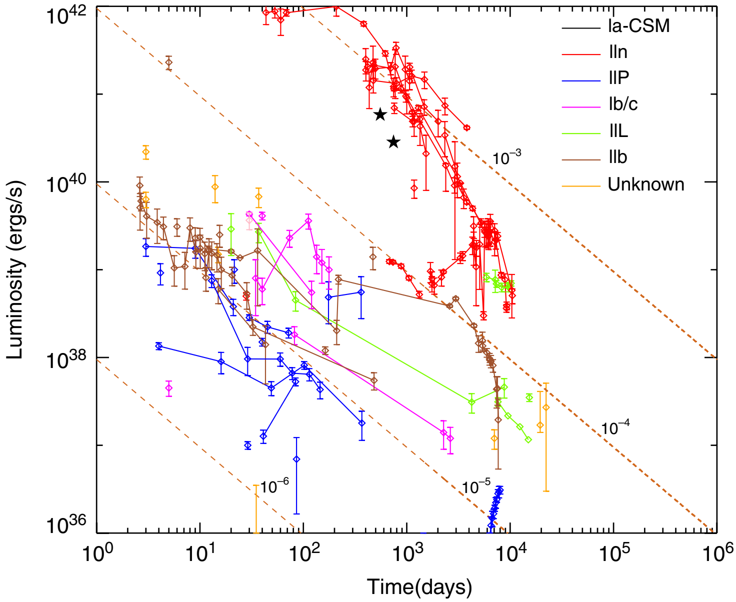

Figure 1. X-Ray Lightcurves of most observed X-Ray SNe. Grouped by type. Dashed lines are lines of constant mass-loss, with t^{-1} slope. Mass-loss rates in $M_\odot$ yr^{-1} assuming wind with constant parameters (density $\propto r^{-2}$), $v_{wind} = 10$ km s^{-1}, electron temperature assumed 10% of the ion temperature behind the shock [Chevalier & Fransson (2003)].

Fig. 1 shows the currently available set of lightcurves. We have grouped them according to the type of SN. Almost all the SNe, barring one, are of the core-collapse variety. The single exception (black stars) is a Type Ia-CSM SN (Bochenek *et al.* 2018). These are a rare and unusual class of SNe (Silverman *et al.* 2013) that show a spectrum very similar to those of a Type Ia SN, but including hydrogen lines (the general characteristic of a Ia is that it has no hydrogen).

We then invert Equation 2.1 to overplot lines of X-ray luminosity at a constant mass-loss rate. We use an electron-to-proton temperature ratio of 0.1 which is generally true for many young SNe, although we caution that at the highest densities, typical of the Type IIn SNe for example, Coulomb equilibration will bring the electron and proton temperatures closer to equilibrium.

The mass-loss rate for any SN can be directly read off the plot. Although these rates are approximate, and sometimes different from what more detailed analysis reveals, the plot reveals several interesting characteristic of the mass-loss rates of various SN types

• *Type IIP SNe* These have the lowest mass-loss rates, in general lower than about 10^{-5} $M_\odot$ yr^{-1}. These mass-loss rates led Dwarkadas (2014) to conclude that the progenitors of Type IIP SNe were red supergiants with initial mass $< 19\,M_\odot$. This result is in agreement with results derived via direct optical measurements (Smartt 2009, Smartt 2015), as well as theoretical calculations (Sukhbold *et al.* 2016).

• *Type IIn SNe* These have the highest mass-loss rates, generally higher than $10^{-4}\,M_\odot$ yr^{-1}, and even exceeding $10^{-3}\,M_\odot$ yr^{-1}. Note however that they show the maximum deviation from the t^{-1} slope of the lightcurves, and consequently from an r^{-2} density profile for the wind medium. This suggests that the mass-loss rate, or wind velocity, or both, are functions of time, and hence radius. The slopes are generally much steeper than t^{-1}. If the wind velocity is assumed constant, as is frequently taken to be the case, then this implies that the mass-loss rates are much higher closer to the onset of core-collapse,

https://doi.org/10.1017/S1743921318008438 Published online by Cambridge University Press

and could significantly exceed even the rates suggested here (see below). If the wind velocity is larger than 10 km s^{-1}, the mass-loss rate will also be correspondingly higher.

• *Type IIL, Type IIb* Although the statistics are low, these have mass-loss rates somewhat higher than the IIPs. If the mass-loss rates increase with stellar mass, these suggest marginally higher mass progenitors for IILs and IIbs as compared to IIPs.

• *Type Ib/c* SNe of Type Ib/c show mass-loss rates that are $> 10^{-5}$ $M_\odot$ yr^{-1}. However, the general assumption is that Type Ib/c SNe arise from Wolf-Rayet stars (due to the lack of H/He in their spectra). The winds of these stars have velocities > 1000 km s^{-1} (Crowther 2007). This implies that the mass-loss rates quoted above must be multiplied by a factor $\geqslant 100$. This would result in mass-loss rates $> 10^{-3}$ $M_\odot$ yr^{-1}, substantially exceeding mass-loss rates for any known Wolf-Rayet stars. The inference may be that the assumption of thermal emission is incorrect. Chevalier & Fransson (2006) have in fact suggested that the emission from Ib/c SNe is non-thermal, due to synchrotron and/or Inverse Compton processes.

4. Accurate determinations of mass-loss rates

Using well-sampled X-ray lightcurves and high resolution X-ray data, it is possible to determine the mass-loss rates of individual SNe much more accurately. This was demonstrated in Fransson *et al.* (1996). Chandra *et al.* (2015) determined a mass-loss rate of 0.06 $M_\odot$ yr^{-1} for SN 2010jl, which agrees well with the optically determined value of 0.1 $M_\odot$ yr^{-1} by Fransson *et al.* (2014). For SN 2005kd, Dwarkadas *et al.* (2016) find a mass-loss rate of 4.3 $\times 10^{-4}$ $M_\odot$ yr^{-1} for a wind velocity of 10 km s^{-1} at 10^{16} cm, and infer that it could have been $> 10^{-3}$ $M_\odot$ yr^{-1} closer to core-collapse. If the wind velocity is higher, as is likely for Type IIn SNe, this mass-loss rate would be even higher.

For the other SN types, the mass-loss rates may be more similar to those deduced from the plot above. Figure 1 suggests a mass-loss rate somewhat greater than 10^{-5} $M_\odot$ yr^{-1} for SN 1993J. This is consistent with the mass-loss rate of 4 $\times 10^{-5}$ $M_\odot$ yr^{-1} deduced by Tatischeff (2009) via fitting of the radio lightcurves of the SN.

5. Conclusions

The X-ray emission from young SNe can be used to deduce the density of the medium into which the SN is expanding, and thus the mass-loss rate of the progenitor star for a medium formed by stellar mass-loss. This can provide insight into the mass-loss rates of massive stars in the years, decades and centuries before core-collapse, which are otherwise difficult to determine. The values so derived agree with those obtained from observations at other wavelengths. They show that Type IIPs are expanding in winds with the lowest mass-loss rates, while IIns have the highest mass-loss rates, which may exceed 10^{-3} $M_\odot$ yr^{-1}, and perhaps higher depending on their wind velocities. It is unclear which progenitor stars could sustain such high mass-loss rates, although luminous blue variable stars have been suggested (Smith 2014).

Acknowledgements

VVDs work on X-ray SNe is supported by NASA Astrophysics Data Analysis program grant # NNX14AR63G awarded to PI V. Dwarkadas at the University of Chicago. We also acknowledge several Chandra grants over the years, including GO1-12095A, GO2-13092B, GO4-15075X and GO7-18066X. VVD would like to thank the IAU for a travel grant that enabled him to attend the 2018 IAU General Assembly.

References

Bauer, F. E., Dwarkadas, V. V., Brandt, W. N., Immler, S., Smartt, S., Bartel, N. & Bietenholz, M. F. 2008, *ApJ*, 688, 1210

https://doi.org/10.1017/S1743921318008438 Published online by Cambridge University Press

Bochenek, C. D., Dwarkadas, V. V., Silverman, J. M., Fox, O. D., Chevalier, R. A.; Smith, N, & Filippenko, A.V. 2018, *MNRAS*, 473, 336
Chakraborti, S., Ray, A., Smith, R., Ryder, S., Yadav, N., Sutaria, F., Dwarkadas, V. V., Chandra, P., Pooley, D., & Roy, R. 2013, *ApJ*, 774, 30
Chakraborti, S., Ray, A., Smith, R., Margutti, R., Pooley, D., Bose, S., Sutaria, F., Chandra, P., Dwarkadas, V.V., Ryder, S., & Maeda, K. 2016, *ApJ*, 817, 22
Chandra, P., Dwarkadas, V. V., Ray, A., Immler, S., & Pooley, D. 2009, *ApJ*, 699, 388
Chandra, P., Chevalier, R. A., Chugai, N., Fransson, C., Irwin, C. M., Soderberg, A. M., Chakraborti, S., & Immler, S. 2012, *ApJ*, 755, 110
Chandra, P., Chevalier, R. A., Chugai, N., Fransson, C., Soderberg, A. M., Chakraborti, S., & Immler, S. 2012, *ApJ*, 810, 32
Crowther, P. A. 2007, *ARAA*, 45, 177
Chevalier, R. A., & Fransson, C. 2003, in: K. Weiler (ed), *Supernovae and Gamma-Ray Bursters, Lecture Notes in Physics*, (Berlin: Springer Verlag), 598, 17
Chevalier, R. A., & Fransson, C. 2006, *ApJ*, 651, 381
Chevalier, R. A., Fransson, C., & Nymark, T. 2006, *ApJ*, 641, 1029
Chevalier, R. A., & Soderberg, A. M. 2010, *ApJ*, 711, L40
Dwarkadas, V. V, & Gruszko, J. 2012, *MNRAS*, 419, 1515
Dwarkadas, V. V., Bauer, F. E., Bietenholz, M., & Bartel, N. 2014, in J-U. Ness (ed), *The X-ray Universe 2014*, 248
Dwarkadas, V. V, 2014, *MNRAS*, 440, 1917
Dwarkadas, V. V., Romero-Caizales, C., Reddy, R., & Bauer, F. E. 2016, *MNRAS*, 462, 1101
Fransson, C., Lundqvist, P., & Chvelier, R. A. 1996, *ApJ*, 461, 993
Fransson, C., Ergon, M., Challis, P. J., Chevalier, R. A., France, K., Kirshner, R. P., Marion, G. H., *et al.* 2014, *ApJ*, 797, 118
Immler, S., Fesen, R. A., Van Dyk, S. D., Weiler, K. W., Petre, R. Lewin, W. H. G., Pooley, D., Pietsch, W., Aschenbach, B., Hammell, M. C., & Rudie, G. C. 2005, *ApJ*, 632, 2381
Patnaude, D. J., Loeb, A., & Jones, C. 2011, *NewA*, 16, 187
Silverman, J. M., Nugent, P. E., Gal-Yam, A., Sullivan, M., Howell, D. A., Filippenko, A. V., *et al.* 2013, *ApJS*, 207, 3
Smartt, S. J. 2009, *ARAA*, 47, 63
Smartt, S. J. 2015, *PASA*, 32, 16
Smith, N. 2014, *ARAA*, 52, 487
Sukhbold, T., Ertl, T., Woosley, S. E., Brown, J. M., & Janka, H.-T. 2016, *ApJ*, 821, 38
Tatischeff, V. 2009, *A&A*, 499, 191